

Distributions of Transition Matrix Elements in Classically Mixed Quantum Systems

Dominique Boosé

Laboratoire de Physique Théorique, Université Louis Pasteur, F-67084 Strasbourg, France

Jörg Main

Institut für Theoretische Physik I, Ruhr-Universität Bochum, D-44780 Bochum, Germany

(May 14, 1999)

The quantitative contributions of a mixed phase-space to the mean characterizing the distribution of diagonal transition matrix elements and to the variance characterizing the distributions of non-diagonal transition matrix elements are studied. It is shown that the mean can be expressed as the sum of suitably weighted classical averages along an ergodic trajectory and along the stable periodic orbits. Similarly, it is shown that the values of the variance are well reproduced by the sum of the suitably weighted Fourier transforms of classical autocorrelation functions along an ergodic trajectory and along the stable periodic orbits. The illustrative numerical computations are done in the framework of the Hydrogen atom in a strong magnetic field, for three different values of the scaled energy.

PACS numbers: 05.45.+b, 03.65.Sq, 32.60.+i, 32.70.Cs

I. INTRODUCTION

It is well known that Random Matrix Theory is able to reproduce successfully statistical properties which characterize the semiclassical regime of quantum systems with a few freedoms having a fully ergodic classical phase-space. This is true for bound systems since the short-ranged spectral statistics, those using energy levels which are separated by some multiples of the mean level spacing, are well described in this approach (see, e.g., Ref. [1]). This is also true for scattering systems since the fluctuations of the S -matrix elements are well modeled with the help of random matrices [2]. The predictions of Random Matrix Theory are universal, that is they are independent of the microscopic details of the particular system under study. It is Classical Mechanics which provides the ultimate justification for universality. For instance, the universal behavior of the spectral statistics is justified by resorting to the principle that the very long unstable periodic orbits of the underlying classical dynamics are uniformly distributed in phase-space (see, e.g., Ref. [3]). For instance also, the universal energy dependence of the S -matrix autocorrelation function is explained by the fact that the distribution in length of the very long unstable scattering trajectories has a generic functional form for classical ergodic systems (see, e.g., Ref. [4]).

Another example of universal behavior has to do with the transition matrix elements associated to an opera-

tor perturbing a quantum system with an ergodic phase-space. Indeed, Random Matrix Theory predicts that these transition matrix elements are independent random variables distributed in a normal way [5]. However, mean and variance characterizing these distributions are free parameters and therefore lack a physical meaning in this approach. In view of the previously given examples, it appears natural to link this other universal property to Classical Mechanics again. This can actually be done by means of the generalization of the semiclassical theory pioneered by Gutzwiller [6,7] to arbitrary (well behaved) operators [8,9], a generalization which allows to give a classical interpretation of mean and variance. Indeed, in the semiclassical limit of Quantum Mechanics, the leading order expression of the mean value of the diagonal transition matrix elements is equal to the microcanonical average of the Weyl transform of the perturbing operator [8,9]. In the same limit, the leading order expression of the variance associated to the Gaussian distributions generated with non-diagonal transition matrix elements is proportional to the Fourier transform of the classical autocorrelation function of the Weyl transform of the perturbing operator [8,9]. The link between classical variance and autocorrelation function has been studied numerically in three quantum systems with an ergodic phase-space, a quartic oscillator [10], an oval billiard [11] and the Hydrogen atom in a strong magnetic field [12]. In these systems and for several examples of perturbing operators, it has actually been found that the autocorrelation function of the Weyl transform of the perturbing operator determines with an excellent accuracy the local values of the classical variance. Moreover, it has been verified [11] that the semiclassical corrections to the leading order expression of the variance which are due to the shortest unstable periodic orbits are in very good quantitative agreement with the theoretical predictions of Refs. [8,9]. The autocorrelation function has also been studied in the framework of a purely regular billiard for two examples of perturbing operators [13]. It has to be added that a method has been proposed [14] to compute the variance associated to the distribution of diagonal transition matrix elements, a quantity which has not been considered in Refs. [8,9]. This method, which rests on periodic orbit theory, has an interesting formal relationship with the supersymmetric methods used in the description of disordered systems [15].

Generic quantum systems with a small number of freedoms d do have a mixed regular-ergodic phase-space.

This means that two different kinds of orbits appear in the underlying classical dynamics. There are orbits which wind regularly round d -dimensional tori and there are orbits which explore densely $(2d - 1)$ -dimensional regions of the energy shell in a highly chaotic manner. Phase-space is therefore naturally partitioned into regular components, each including infinitely many neighboring tori, and ergodic components which are free of tori. These various components are mutually independent. Since Random Matrix Theory appears to be relevant to quantum systems with a fully ergodic phase-space exclusively, the previously listed universal properties do not hold anymore for quantum systems with a mixed phase-space. However, one may still wonder about the presence in statistical properties pertaining to mixed quantum systems of fingerprints related to the coexistence of regular and ergodic regions in phase-space. Berry and Robnik [16] have been among the first to tackle this question. Assuming that the semiclassical spectrum of a mixed quantum system is the superposition of statistically independent sequences of levels from each of the phase-space components, they have deduced a semi-phenomenological closed formula for the level spacing distribution. The formula makes use of the total phase-space volume of all regular regions as well as of the individual phase-space volumes of all ergodic regions. Their line of argument has been extended to other spectral statistics [17]. The validity of the semi-phenomenological formulae obtained for the spectral statistics has been supported by numerical computations [17]. Apart from the one of Berry and Robnik [16], two other parametrizations of the level spacing distribution have been proposed to characterize a mixed quantum system. These are the parametrizations of Brody [18] and of Izrailev [19], whose validity has also been supported by numerical computations. The link between the mixed character of phase-space and statistical properties of transition matrix elements has been studied by Robnik and Prosen [20,21]. Extending to eigenvectors the assumption of independent sequences originally proposed for energy levels, they have argued that the only transition matrix elements which have to be considered in the semiclassical limit are those whose initial and final states can be associated to the same component of phase-space. Moreover, they have generalized the results of Refs. [8,9] by showing that the expression of the variance characterizing the distributions of non-diagonal transition matrix elements whose initial and final states can be associated to a given component of phase-space (which is either an ergodic region or some set of quantized tori lying closely together) always involves a microcanonical average over this very component. Numerical computations [20,21] have corroborated the validity of their results.

The purpose of the present paper is to provide a detailed study of the quantitative contributions coming from the various components of a mixed phase-space to the mean characterizing the distribution of diagonal transition matrix elements and to the variance characterizing the distributions of non-diagonal transition matrix ele-

ments. It means in particular to complement the study of Robnik and Prosen on a specific aspect of the link between the mixed character of phase-space and statistical properties of transition matrix elements which was not considered by them. This aspect concerns the use of the stable periodic orbits in the computation of the quantitative contributions coming from the various regular components of phase-space to the values of mean and variance. The study of this particular point is interesting because of the two following reasons. On the one hand, the method proposed in Refs. [20,21] to compute the variance is not easy to use in practice since it requires the prior identification in phase-space of the adequate neighboring quantized tori. On the other hand, a given stable periodic orbit is in a way able all alone to account for the quantitative contribution of its associated regular component to the semiclassical density of states [22,23,7]. Considering these two facts, one may wonder whether stable periodic orbits (whose practical identification is usually easier than the one of specific quantized tori) cannot help to compute in a convenient way the quantitative contributions of the regular regions to the values of mean and variance. The paper shows that this is indeed the case by providing closed formulae for mean and variance in which stable periodic orbits are involved. Such formulae generalize to the case of mixed quantum systems those studied in Refs. [8,9,11,12]. This work extends the one of Ref. [24] where details have been omitted because of lack of space. The illustrative numerical computations are again done in the framework of the Hydrogen atom in a strong magnetic field.

The paper is organized as follows. In Section II, some details relating to the scaling property which characterizes the Hydrogen atom in a strong magnetic field are given and the choice of the perturbing operator used for the numerical computation of the transition matrix elements is justified. Section III deals with the mean value of the distribution of diagonal transition matrix elements, a quantity which was not considered in Refs. [20,21]. The quantitative contributions of the ergodic and regular regions making up the mixed phase-space are identified. The contributions of the various regular components are calculated with the help of the associated stable periodic orbits. The illustrative numerical computations are done for three different values of the scaled energy. Section IV is concerned with the variance characterizing the distributions of non-diagonal transition matrix elements. First, the orders of magnitude of the transition probabilities whose initial and final states are referring or not to the same phase-space component are compared. The quantitative contributions to the variance of the ergodic and regular regions are then studied. The manner in which a given stable periodic orbit is used in the calculation of the contribution coming from the associated regular component is discussed. The illustrative numerical computations are done for the same values of the scaled energy as in the previous section. A Conclusion summarizes the main results of the paper.

II. SCALING AND TRANSITION MATRIX ELEMENTS

To begin with, it is not an easy task to study the quantitative effect of the underlying classical dynamics on the statistical properties of transition matrix elements. This is due to the fact that the structure of phase-space changes with energy for most systems. Consequently, any diagonal transition matrix element $\langle m|\hat{A}|m\rangle$ ($|m\rangle$ being an eigenvector of the system and \hat{A} the perturbing operator) is usually going with a different energy shell. The problem becomes even trickier when considering non-diagonal transition matrix elements $\langle m|\hat{A}|n\rangle$ since initial and final eigenstates are always going with different energy shells. The study should therefore be done using a set of transition matrix elements in which initial and final eigenenergies are restricted to an energy interval small enough for phase-space to keep its structure practically unchanged. However, in order to get a significant number of transition matrix elements, one should choose an energy region which is high enough in the spectrum so that the density of states can make up for the smallness of the used energy interval. This would obviously require the diagonalization of very large matrices in practice. Such numerical difficulties can be avoided by studying scaling systems. These are systems possessing scaling properties which imply that phase-space has the same structure at all energies. The Hydrogen atom in a strong magnetic field [25] and the three-body Coulomb system [26] are physically interesting examples of scaling systems. The Hamiltonian of a scaling system depends on a scaling parameter. It is useful to follow the variation of the energy levels with the scaling parameter [25,26] since one can extract informations about the underlying classical dynamics from spectra taken at different values of the scaling parameter by application of the so-called method of scaled energy spectroscopy [27,28].

In atomic units, the quantum Hamiltonian of the Hydrogen atom in a strong magnetic field reads [25]

$$\hat{H}_\gamma(\hat{\mathbf{p}}, \hat{\mathbf{r}}) = \frac{1}{2}\hat{\mathbf{p}}^2 - \frac{1}{\hat{r}} + \frac{1}{2}\gamma\hat{L}_z + \frac{1}{8}\gamma^2(\hat{x}^2 + \hat{y}^2). \quad (1)$$

Here \hat{L}_z is the component of the angular momentum operator along the direction of the magnetic field. This component is conserved and, consequently, the azimuthal quantum number m is a good quantum number. Numerical computations are restricted to the subspace $m = 0$ in this study. The Hamiltonian is invariant under reflection with respect to the plane which is perpendicular to the direction of the magnetic field and the z -parity π_z is thereby a good quantum number too. The parameter γ is the magnetic field strength in atomic units, $\gamma = B/(2.35 \times 10^5 \text{ T})$. When expressed in terms of the scaled coordinates $\tilde{\mathbf{r}} = \gamma^{2/3}\mathbf{r}$ and scaled momenta $\tilde{\mathbf{p}} = \gamma^{-1/3}\mathbf{p}$, the classical Hamiltonian scales as

$$\tilde{H}_{\gamma=1}(\tilde{\mathbf{p}}, \tilde{\mathbf{r}}) = \frac{1}{2}\tilde{\mathbf{p}}^2 - \frac{1}{\tilde{r}} + \frac{1}{2}\tilde{L}_z + \frac{1}{8}(\tilde{x}^2 + \tilde{y}^2)$$

$$= \gamma^{-2/3}H_\gamma(\mathbf{p}, \mathbf{r}) = \gamma^{-2/3}E = \tilde{E}, \quad (2)$$

with E the excitation energy. Therefore, the classical dynamics obtained from the scaled equations of motion does not depend on E and γ independently but on a single parameter combining both physical quantities, the scaled energy $\tilde{E} = \gamma^{-2/3}E$. This implies that the structure of phase-space is identical for any pair (E, γ) leading to the same value of the scaled energy.

If \hat{z} and \hat{p}_z are the scaled coordinate and momentum operators along the direction of the magnetic field, one has $[\hat{z}, \hat{p}_z] = i\gamma^{1/3}\hbar$ by virtue of the previously given definition of scaled variables. The dependence of the quantum dynamics on the magnetic field strength γ can thereby be taken into account by means of an effective Planck's constant $\hbar_{\text{eff}} = \gamma^{1/3}\hbar$ ($\hbar = 1$ subsequently). One approaches the semiclassical limit at constant scaled energy $\hbar_{\text{eff}} \rightarrow 0$ by decreasing the value of γ . The quantization of Eq. (2) in the subspace $m = 0$ leads to a generalized eigenvalue equation for the scaling parameter $w = \gamma^{-1/3} = \hbar_{\text{eff}}^{-1}$. The introduction of the scaled semi-parabolic coordinates $\tilde{\mu} = \sqrt{\tilde{r} + \tilde{z}}$ and $\tilde{\nu} = \sqrt{\tilde{r} - \tilde{z}}$ allows to write this generalized eigenvalue equation as

$$\left[2\tilde{E}(\tilde{\mu}^2 + \tilde{\nu}^2) - \frac{1}{4}\tilde{\mu}^2\tilde{\nu}^2(\tilde{\mu}^2 + \tilde{\nu}^2) + 4 \right] \Psi(\tilde{\mu}, \tilde{\nu}) = w^{-2} \left(\hat{p}_\mu^2 + \hat{p}_\nu^2 \right) \Psi(\tilde{\mu}, \tilde{\nu}), \quad (3)$$

with the radial operators \hat{p}_μ^2 and \hat{p}_ν^2 defined as

$$\hat{p}_\mu^2 = -\frac{1}{\tilde{\mu}} \frac{\partial}{\partial \tilde{\mu}} \left(\tilde{\mu} \frac{\partial}{\partial \tilde{\mu}} \right), \quad \hat{p}_\nu^2 = -\frac{1}{\tilde{\nu}} \frac{\partial}{\partial \tilde{\nu}} \left(\tilde{\nu} \frac{\partial}{\partial \tilde{\nu}} \right).$$

Eq. (3) can be written in matrix form by using the complete set of basis functions which is composed of the tensorial products of the eigenvectors of two uncoupled two-dimensional harmonic oscillators with frequency $\sqrt{-2\tilde{E}}$ [25,29]. The generalized eigenvalue equation is solved with the help of the Lanczos spectral transformation method, which is adapted to the diagonalization of sparse symmetric matrices [30]. One obtains in this way the spectrum of eigenvectors $|\Psi_m\rangle$ and corresponding eigenvalues $w_m = (\gamma^{-1/3})_m$. The structure of phase-space is the same at every eigenenergy w_m since the generalized eigenvalue equation has been solved at constant scaled energy \tilde{E} . Consequently, the matrix elements describing the various transitions caused in the spectrum by a perturbing operator are all going with the same underlying classical dynamics. It has to be noted that the eigenvectors $|\Psi_m\rangle$ are not orthogonal. However, the modified eigenvectors $|m\rangle = \sqrt{\hat{p}_\mu^2 + \hat{p}_\nu^2}|\Psi_m\rangle$ (with the same corresponding eigenvalues w_m) are orthogonal, i.e.

$$\langle m|n\rangle = \langle \Psi_m | \hat{p}_\mu^2 + \hat{p}_\nu^2 | \Psi_n \rangle = \delta_{mn}. \quad (4)$$

The perturbing operator which has been chosen for this study is

$$\hat{A} = \frac{1}{2r\hat{\mathbf{p}}^2} = \frac{w^2}{\hat{p}_\mu^2 + \hat{p}_\nu^2}. \quad (5)$$

The second expression in this equation is the effective expression of the operator \hat{A} when acting onto eigenvectors belonging to the subspace $m = 0$. The same operator has been used in previous papers [12,24] already. The reason is that this particular operator is convenient to handle in practice since the general expression of the associated transition matrix elements in the orthonormal basis $\{|m\rangle\}$ of modified eigenvectors is

$$\langle m|\hat{A}|n\rangle = w_m w_n \langle \Psi_m|\Psi_n\rangle. \quad (6)$$

The computation of the transition matrix elements at constant scaled energy amounts therefore merely to the computation of the various overlaps of the eigenvectors $\{|\Psi_m\rangle\}$. Moreover, this computation can be restricted to a subspace which is labeled by a given value of π_z because the operator \hat{A} connects only eigenstates of the same z -parity. Numerical computations are done here in the subspace $m^\pi = 0^+$. This special perturbing operator offers another computational advantage. Indeed, it turns out that the average at constant scaled energy of the Weyl transform \tilde{A} of the operator \hat{A} along a given trajectory in phase-space has an analytic expression, given in Eq. (10) below. This average, which is important for the physical interpretation of the numerical results presented in this paper, can therefore be computed accurately. The Weyl transform of the perturbing operator is expressed most simply with the help of the scaled semi-parabolic momenta \tilde{p}_μ and \tilde{p}_ν , the conjugate variables of the scaled semi-parabolic coordinates $\tilde{\mu}$ and $\tilde{\nu}$. These momenta are defined as the derivatives of the coordinates $\tilde{\mu}$ and $\tilde{\nu}$ with respect to the so-called rescaled time variable τ [25]. The expression of \tilde{A} is

$$\tilde{A}(\tilde{p}_\mu, \tilde{p}_\nu) = \frac{1}{\tilde{p}_\mu^2 + \tilde{p}_\nu^2}. \quad (7)$$

The scaling parameter $w = \gamma^{-1/3}$ and the scaled action $\tilde{s}(\tilde{E}) = \int (\tilde{p}_\mu d\tilde{\mu} + \tilde{p}_\nu d\tilde{\nu})$ are conjugate variables at constant scaled energy. Since the variable w is an energy variable, the variable \tilde{s} can be considered as a time variable which measures the length of trajectories in the four-dimensional phase-space spanned by the scaled semi-parabolic variables $(\tilde{\mu}, \tilde{\nu}, \tilde{p}_\mu, \tilde{p}_\nu)$ [31]. The infinitesimal scaled action $d\tilde{s}$ and the infinitesimal rescaled time $d\tau$ are linked together by the relation

$$d\tilde{s} = \tilde{p}_\mu d\tilde{\mu} + \tilde{p}_\nu d\tilde{\nu} = (\tilde{p}_\mu^2 + \tilde{p}_\nu^2) d\tau. \quad (8)$$

This relation implies that the Weyl transform \tilde{A} can be expressed at constant scaled energy as the derivative of the variable τ with respect to the variable \tilde{s} , i.e.

$$\tilde{A}(\tilde{p}_\mu, \tilde{p}_\nu) = \frac{d\tau}{d\tilde{s}} = \tilde{A}(\tilde{s}). \quad (9)$$

The average at scaled energy \tilde{E} of the Weyl transform \tilde{A} along a trajectory with scaled action $S(\tilde{E})$ corresponding to a total rescaled time τ is then simply

$$\frac{1}{S(\tilde{E})} \int_0^{S(\tilde{E})} d\tilde{s} \tilde{A}(\tilde{s}) = \frac{1}{S(\tilde{E})} \int_0^\tau d\tau = \frac{\tau}{S(\tilde{E})}. \quad (10)$$

III. DIAGONAL TRANSITION MATRIX ELEMENTS

This section studies the quantitative contributions coming from the ergodic and regular components of the mixed phase-space to the mean value characterizing the distribution of diagonal transition matrix elements associated to the perturbing operator \hat{A} . The study is done for three successive values of the scaling energy \tilde{E} , which are $\tilde{E} = -0.2$, $\tilde{E} = -0.316$ and $\tilde{E} = -0.4$. Fig. 1 displays the Poincaré surfaces of section for these different cases in the scaled semiparabolic representation $(\tilde{\mu}, \tilde{p}_\mu; \tilde{\nu} = 0)$. In the case $\tilde{E} = -0.2$ (Fig. 1a), the surface of section has two islands of stable motion which are embedded in a simply connected ergodic sea. Both islands belong to the same regular component since they are conjugate with

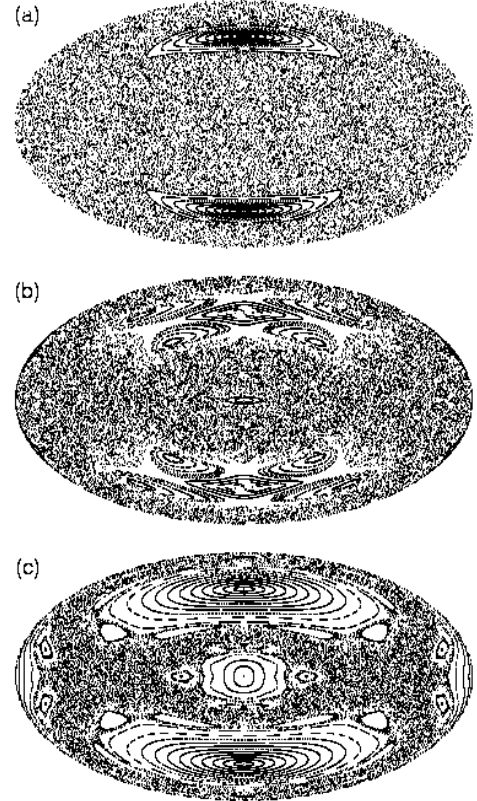


FIG. 1. Poincaré surfaces of section of the Hydrogen atom in a strong magnetic field in the scaled semi-parabolic representation $(\tilde{\mu}, \tilde{p}_\mu; \tilde{\nu} = 0)$ for three different values of the scaled energy \tilde{E} . (a) $\tilde{E} = -0.2$; (b) $\tilde{E} = -0.316$; (c) $\tilde{E} = -0.4$.

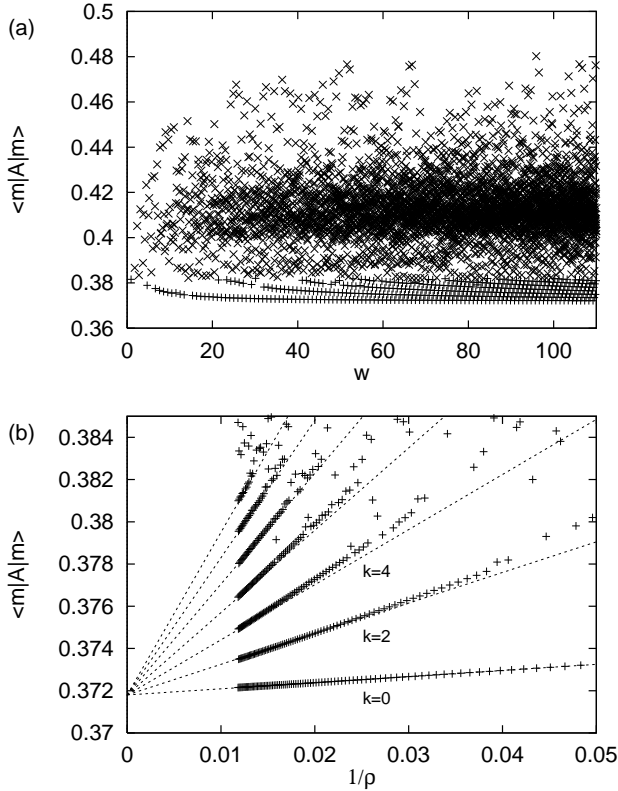


FIG. 2. Distribution of values of the diagonal transition matrix elements $\langle m|\hat{A}|m\rangle$ corresponding to the operator $\hat{A} = 1/2r\hat{\mathbf{p}}^2$ in the case of the scaled energy $\tilde{E} = -0.2$. (a) Distribution of values of the matrix elements associated to the chaotic (\times) and regular ($+$) states as a function of the scaling parameter w ; (b) Distribution of values of the matrix elements associated to the regular states as a function of the inverse of the mean total density of states $\rho_{0,t}(w)$.

respect to the line $\tilde{p}_\mu = 0$. This regular component is associated to a stable periodic orbit lying in the plane perpendicular to the direction of the magnetic field, with scaled action $S_r = 6.49086$. Fig. 2a displays, for the same value of the scaling energy, the distribution of values of the diagonal transition matrix elements as a function of the scaling parameter $w = \gamma^{-1/3} = \hbar_{\text{eff}}^{-1}$. This figure shows clearly the presence of two different patterns. On the one hand, there appears a statistical distribution built up with diagonal transition matrix elements which are represented by "x" symbols. A further analysis reveals that these matrix elements involve eigenstates whose Husimi distribution [32] is essentially localized within the ergodic sea. Such eigenstates are called "chaotic" in the sequel. They are generically labelled as $|m_c\rangle$, with corresponding eigenvalues $w_m^{(c)}$. These eigenvalues belong to a subset of the spectrum which is characterized by a mean density of states $\rho_{0,c}(w) = 0.702w$. On the other hand, one distinguishes in the lower part of Fig. 2a several sequences of diagonal matrix elements which are represented by "+" symbols. The Husimi distributions of the corresponding eigenstates are well localized

within the two islands of stable motion in Fig. 1a. Such eigenstates are called "regular" in the sequel. They are generically labelled as $|m_r\rangle$, with corresponding eigenvalues $w_m^{(r)}$. These eigenvalues belong to a subset of the spectrum which is complementary to the previous one and whose mean density of states is $\rho_{0,r}(w) = 0.066w$. The coexistence of these two different patterns of diagonal transition matrix elements illustrates well the fact that the spectrum of a mixed quantum system can be split into independent subsets of eigenvectors, each of which going with a different component of phase-space [16].

The quantitative interpretation of Fig. 2a is done with the help of a scaled spectral function $D(w)$ which takes all diagonal matrix elements of the perturbing operator \hat{A} into account. It is defined as

$$D(w) = \sum_m \langle m|\hat{A}|m\rangle \delta(w - w_m). \quad (11)$$

According to Refs. [8,9], the semiclassical expression of $D(w)$ which is relevant to the fully ergodic case is

$$D(w) = \frac{w^4}{(2\pi)^2} \int_{\Omega} d\tilde{p}_\mu d\tilde{p}_\nu d\tilde{\mu} d\tilde{\nu} (\tilde{\mu}^2 + \tilde{\nu}^2) \times \tilde{A}(\tilde{p}_\mu, \tilde{p}_\nu) \delta(\tilde{H}(\tilde{p}_\mu, \tilde{p}_\nu, \tilde{\mu}, \tilde{\nu}) - 2) + \frac{1}{\pi} \sum_{\{p\}} A_p \sum_{s=1}^{\infty} \frac{\sin\left(s\left(wS_p(\tilde{E}) - \alpha_p\pi/2\right)\right)}{[\det(M_p^s - I)]^{1/2}}, \quad (12)$$

with

$$\tilde{H}(\tilde{p}_\mu, \tilde{p}_\nu, \tilde{\mu}, \tilde{\nu}) = \frac{1}{2} (\tilde{p}_\mu^2 + \tilde{p}_\nu^2) - (\tilde{\mu}^2 + \tilde{\nu}^2)\tilde{E} + \frac{1}{8}\tilde{\mu}^2\tilde{\nu}^2(\tilde{\mu}^2 + \tilde{\nu}^2). \quad (13)$$

The expression of $D(w)$ is written here in the scaled semiparabolic representation of phase-space. The first term on the r.h.s. of Eq. (12), the so-called Weyl term, gives the classical contribution to the scaled spectral function. It factorizes into two parts as a consequence of the use of the scaled semiparabolic representation. One part depends solely on the scaling parameter w whereas the other part, which involves a phase-space integration over the whole energy shell Ω at constant scaled energy \tilde{E} , is independent of it. The second term gives the leading order corrections to the Weyl term in an asymptotic expansion of $D(w)$ into powers of \hbar . These corrections are generated by the periodic orbits of the underlying classical dynamics, which are all unstable. The outer sum in the second term runs over the set $\{p\}$ of all primitive periodic orbits whereas the inner sum runs over all repetitions s of every primitive periodic orbit. Each primitive periodic orbit p is characterized by an amplitude A_p whose expression is

$$A_p = \oint d\tilde{s} \tilde{A}(\tilde{s}). \quad (14)$$

In this equation, the integration is done along the considered periodic orbit and over one period $S_p(\tilde{E}) = \oint(\tilde{p}_\mu d\tilde{\mu} + \tilde{p}_\nu d\tilde{\nu})$. The scaled action $S_p(\tilde{E})$ appears in the argument of the sine function together with the scaling parameter w since it scales as $S_p(\tilde{E}) = w^{-1}S_p(E)$, $S_p(E)$ being the usual action computed at the excitation energy $E = \tilde{E}/w^2$. Every primitive periodic orbit is also characterized by its monodromy matrix M_p and its Maslov index α_p , which are both independent of energy for scaling systems. The importance of the correction due to the s -th repetition of the primitive periodic orbit p depends on the determinant of the difference between the s -th power of M_p and the unit matrix I . As Fig. 2a shows, the scaled spectral function $D(w)$ can be written as the sum of two different contributions in the case of a mixed system, i.e.,

$$D(w) = D_c(w) + D_r(w) \quad (15)$$

with

$$D_{c(r)} = \sum_{m_{c(r)}} \langle m_{c(r)} | \hat{A} | m_{c(r)} \rangle \delta(w - w_m^{(c(r))}). \quad (16)$$

The semiclassical expression of $D_c(w)$ (resp. $D_r(w)$), the scaled spectral function which is associated to the ergodic (resp. regular) component of phase-space, is similar to the one given in Eq. (12). The integration in the Weyl term is now done over the corresponding part of the energy shell at constant scaled energy. The leading order corrections to the Weyl term are due to the unstable ($D_c(w)$) or stable ($D_r(w)$) periodic orbits of the underlying classical dynamics.

The semiclassical expression of $D_c(w)$ predicts that the classical contribution to the mean value $\langle \hat{A} \rangle_c$ which characterizes the distribution of diagonal transition matrix elements corresponding to the chaotic eigenstates is given by the microcanonical average of the operator \hat{A} over the ergodic part Ω_c of the energy shell [8,9], i.e.,

$$\langle \hat{A} \rangle_c = \frac{\int_{\Omega_c} d\tilde{p}_\mu d\tilde{p}_\nu d\tilde{\mu} d\tilde{\nu} (\tilde{\mu}^2 + \tilde{\nu}^2) \tilde{A}(\tilde{p}_\mu, \tilde{p}_\nu) \delta(\tilde{H} - 2)}{\int_{\Omega_c} d\tilde{p}_\mu d\tilde{p}_\nu d\tilde{\mu} d\tilde{\nu} (\tilde{\mu}^2 + \tilde{\nu}^2) \delta(\tilde{H} - 2)}, \quad (17)$$

with $\tilde{H}(\tilde{p}_\mu, \tilde{p}_\nu, \tilde{\mu}, \tilde{\nu})$ defined in Eq. (13) [33]. This formula is not easy to use in practice for the computation of the classical contribution since it requires the numerical calculation of three-dimensional phase-space integrals. However, just as in Refs. [11,12], the ergodic theorem allows to replace the microcanonical average with a time (i.e. scaled action) average of the Weyl transform of the perturbing operator along any trajectory exploring the ergodic part of the energy shell in a uniform way. With the help of Eq. (10), the classical contribution to the mean value $\langle \hat{A} \rangle_c$ can be finally expressed as

$$\langle \hat{A} \rangle_c = \lim_{S \rightarrow \infty} \frac{1}{S} \int_0^S d\tilde{s} \tilde{A}(\tilde{s}) = \lim_{S \rightarrow \infty} \frac{\tau(S)}{S}, \quad (18)$$

$\tau(S)$ being the total rescaled time corresponding to the scaled action S . The ergodic theorem ensures that the limit on the r.h.s. of this equation is well defined and unique. This formula is well suited for the numerical calculation of the classical contribution to the mean value. In the case $\tilde{E} = -0.2$, it gives the value $\langle \hat{A} \rangle_c = 0.41$, which is in good agreement with the value 0.411 obtained from the statistical distribution of Fig. 2a. Eq. (18) can therefore be used to compute with an excellent precision the mean value characterizing the distribution of diagonal matrix elements associated to the chaotic eigenstates.

Fig. 2a suggests that all sequences of diagonal matrix elements which correspond to the regular eigenstates are converging towards the same limit as the scaling parameter w increases. This is indeed the case, as clearly shown by Fig. 2b. In this figure, the values of the diagonal matrix elements pertaining to the seven sequences of the previous figure are represented as a function of the inverse of the mean total density of states $\rho_{0,t}(w) = \rho_{0,c}(w) + \rho_{0,r}(w)$. Such a representation is useful since it allows to extrapolate the values of the individual diagonal matrix elements in the semiclassical regime. This comes from the fact that the mean total density of states is proportional to w in the case of the Hydrogen atom in a strong magnetic field ($\rho_{0,t} = 0.768w$ in the case $\tilde{E} = -0.2$), and so its inverse is proportional to the effective Planck's constant $\hbar_{\text{eff}} = \gamma^{1/3}$ of this system. The semiclassical limit at constant scaled energy $\hbar_{\text{eff}} \rightarrow 0$ is therefore reached as $1/\rho_{0,t}(w) \rightarrow 0$. One sees that the values of the diagonal matrix elements in the sequences are approximated all the better by a common limiting value $\langle \hat{A} \rangle_r$ as one comes closer to the semiclassical regime. This behavior is in sharp contrast with the one of the diagonal matrix elements corresponding to the chaotic eigenstates, which are distributed statistically around the mean value $\langle \hat{A} \rangle_c$. The limiting value $\langle \hat{A} \rangle_r$ can be most easily computed by using an expression of the scaled spectral function $D_r(w)$ which is obtained by resumming formally the leading order corrections to the Weyl term generated by the stable periodic orbit and all its repetitions in the following way [23,6,7]. The expression of these corrections for a particular stable periodic orbit r is [23,6,7]

$$- \frac{i}{\pi} A_r \sum_{s=1}^{\infty} \frac{\exp(iswS_r(\tilde{E}) - \alpha_r\pi/2)}{2 \sin(s\pi\gamma_r)}. \quad (19)$$

Here γ_r is the winding number of the stable orbit, which is independent of energy for scaling systems. After expansion of the sine function in the denominator and the subsequent use of the Poisson summation formula, this expression can be rewritten as

$$A_r \sum_{n,k} \delta \left(wS_r(\tilde{E}) - 2\pi \left(n + \frac{\alpha_r}{4} \right) - 2\pi \left(k + \frac{1}{2} \right) \gamma_r \right). \quad (20)$$

This is a formal expression of the scaled spectral function $D_r(w)$ in the semiclassical regime. It predicts that

the semiclassical spectrum of the regular states is similar to the spectrum of a two-dimensional harmonic oscillator [23,6,7]. One direction of harmonic motion is along the stable periodic orbit, whereas the other direction of harmonic motion is transverse to it. This motion takes place on neighboring tori surrounding the orbit. Each such torus is identified by two quantized scaled actions, the action $\tilde{I}_n = 2\pi(n + \alpha_r/4)$ which is associated to the longitudinal motion and the action $\tilde{I}_k = 2\pi(k + 1/2)\gamma_r$ which is associated to the transverse motion [34]. Every regular state is therefore labelled by two quantum numbers n and k . The range of values of both quantum numbers is bounded in practice as a consequence of the finite size of the corresponding region of stable motion [35]. It has been checked that all regular eigenstates building up a given sequence of diagonal matrix elements in Figs. 2a,b are labelled by the same quantum number k . This quantum number is even as a result of the parity symmetry with respect to the plane perpendicular to the direction of the magnetic field. The lowest sequence corresponds to $k = 0$, the next one to $k = 2$ and so on until the last identified sequence which corresponds to $k = 12$. Fig. 2b shows that there are a few diagonal matrix elements which do not belong to any sequence. It has been checked that all of them correspond to regular eigenstates which are involved in quasi-crossings and so cannot be labelled by a fixed value of k . The quantum number n differentiates the regular eigenstates which are associated to a given sequence. The previous formal expression of the scaled spectral function $D_r(w)$ predicts also that the limiting value $\langle \hat{A} \rangle_r$ of the sequences is proportional to the amplitude A_r of the stable periodic orbit, whose expression is given by Eq. (14). The amplitude A_r has to be divided by the scaled action S_r of the orbit for the purpose of normalization. With the help of Eq. (10), this limiting value can be expressed as

$$\langle \hat{A} \rangle_r = \frac{1}{S_r} \oint d\tilde{s} \tilde{A}(\tilde{s}) = \frac{\tau_r}{S_r}, \quad (21)$$

τ_r being the total rescaled time corresponding to the scaled action S_r . It has to be remarked that the classical contribution $\langle \hat{A} \rangle_c$ to the mean characterizing the distribution of diagonal matrix elements associated to the chaotic eigenstates, Eq. (18), and the classical limiting value $\langle \hat{A} \rangle_r$ of the sequences of diagonal matrix elements corresponding to the regular eigenstates, Eq. (21), have similar expressions. Each expression makes use of the classical trajectory which is related to the component of phase-space going with the studied subset of diagonal matrix elements. In the case $\tilde{E} = -0.2$, the scaled action corresponds to a total rescaled time $\tau_r = 2.4135$. This gives the value $\langle \hat{A} \rangle_r = 0.372$ which, as seen in Fig. 2b, agrees very well with the value obtained as the common intersection of the dashed lines interpolating the values of the diagonal matrix elements as one goes towards the semiclassical limit.

Since the total distribution of diagonal matrix elements

is composed of two different subsets corresponding to the two different components of phase-space, its mean value $\langle \hat{A} \rangle_t$ is expected to be the sum of two properly weighted contributions. The contribution which comes from the mean value $\langle \hat{A} \rangle_c$ (resp. limiting value $\langle \hat{A} \rangle_r$) is weighted by the ratio of the mean density of states of the subset of chaotic (resp. regular) states to the mean total density of states. Each weighting factor is roughly equal to the relative volume of the corresponding component of phase-space. The expected expression of $\langle \hat{A} \rangle_t$ is therefore the following

$$\langle \hat{A} \rangle_t = \left(\frac{\rho_{0,c}(w)}{\rho_{0,t}(w)} \right) \langle \hat{A} \rangle_c + \left(\frac{\rho_{0,r}(w)}{\rho_{0,t}(w)} \right) \langle \hat{A} \rangle_r. \quad (22)$$

In the case $\tilde{E} = -0.2$, this formula gives the value $\langle \hat{A} \rangle_t = 0.407$, which is very close from the value $\langle \hat{A} \rangle_t = 0.409$ obtained from the whole distribution of Fig. 2a. Consequently, Eq. (22) allows to calculate with an excellent precision the mean value characterizing the total distribution of diagonal matrix elements. It generalizes to the case of a scaled system with a mixed phase-space the expression of the mean value given in Refs. [8,9] for a scaled system with an ergodic phase-space.

It is expected that there are as many limiting values $\langle \hat{A} \rangle_r$ as there are regular components in phase-space. This important point can be checked by studying the distribution of diagonal matrix elements for values of the scaled energy for which several stable periodic orbits are present in the underlying classical dynamics. This is done in the cases $\tilde{E} = -0.316$ and $\tilde{E} = -0.4$. The Poincaré surface of section corresponding to the first case is displayed in Fig. 1b. There are five islands of stable motion on both sides of the line $\tilde{p}_\mu = 0$, a central island surrounded by a chain of four islands. The two conjugate central islands belong to the same regular component which, as in the case $\tilde{E} = -0.2$, is associated to a stable periodic orbit lying in the plane perpendicular to the direction of the magnetic field. This orbit has a scaled action $S_{r1} = 7.903534$, corresponding to a total rescaled time $\tau_{r1} = 3.108460$. The shape of this orbit is depicted in the semi-parabolic coordinate representation $(\tilde{\mu}, \tilde{\nu})$ in the lower inset of Fig. 3b. The two conjugate chains of four islands of stable motion surrounding the central islands belong to another regular component. The associated stable periodic orbit has a scaled action $S_{r2} = 12.158133$, corresponding to a total rescaled time $\tau_{r2} = 5.028604$. The shape of this orbit is depicted in the scaled semi-parabolic coordinate representation $(\tilde{\mu}, \tilde{\nu})$ in the upper inset of Fig. 3b. Fig. 1c shows the Poincaré surface of section corresponding to the case $\tilde{E} = -0.4$. As in the two previous cases, the two conjugate islands of stable motion on both sides of the line $\tilde{p}_\mu = 0$ belong to a regular component with a stable periodic orbit lying in the plane perpendicular to the direction of the magnetic field. This orbit has a scaled action $S_{r1} = 7.02481$ corresponding to a total rescaled time $\tau_{r1} = 2.866$. The stable island in the middle of the surface of section pertains to

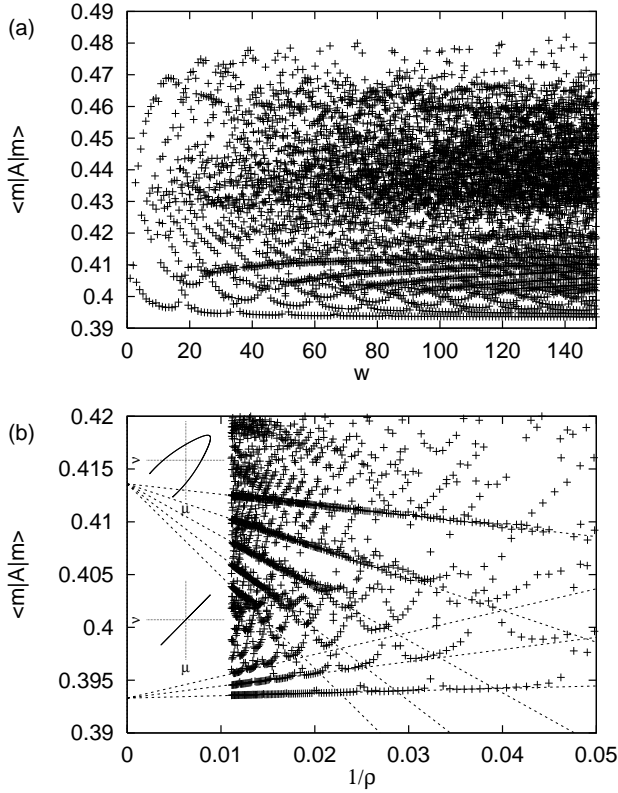


FIG. 3. Same as Fig. 2 but in the case of the scaled energy $\tilde{E} = -0.316$. The shapes of the two stable periodic orbits which are used in the analysis of this case are shown in the insets.

another regular component, with a stable periodic orbit which is parallel to the direction of the magnetic field. This orbit has a scaled action $S_{r2} = 5.791216$, corresponding to a total rescaled time $\tau_{r2} = 2.896$.

Fig. 3a (resp. Fig. 4a) displays the distribution of values of the diagonal matrix elements as a function of the scaling parameter w in the case $\tilde{E} = -0.316$ (resp. $\tilde{E} = -0.4$). Just as in the case $\tilde{E} = -0.2$, the whole distribution results from the juxtaposition of a statistical distribution connected to the ergodic component of phase-space and a set of sequences connected to the regular components of phase-space. These sequences fall into two different groups, as the fingerprint of the existence of two different stable periodic orbits. This is particularly clear in Fig. 4a, where each group of sequences is on a different side of the statistical distribution. In the case $\tilde{E} = -0.4$, the long streaks of diagonal matrix elements appearing in the statistical distribution are presumably the mark of one or several other regular components, which are associated to the small islands of stable motion surrounding the three main islands in Fig. 1c. As previously explained, the identification of the group of sequences linked to a particular regular component is most easily done by representing the values of the diagonal matrix elements in all sequences as a function of the inverse of the mean total density of states $\rho_{0,t}(w)$. This

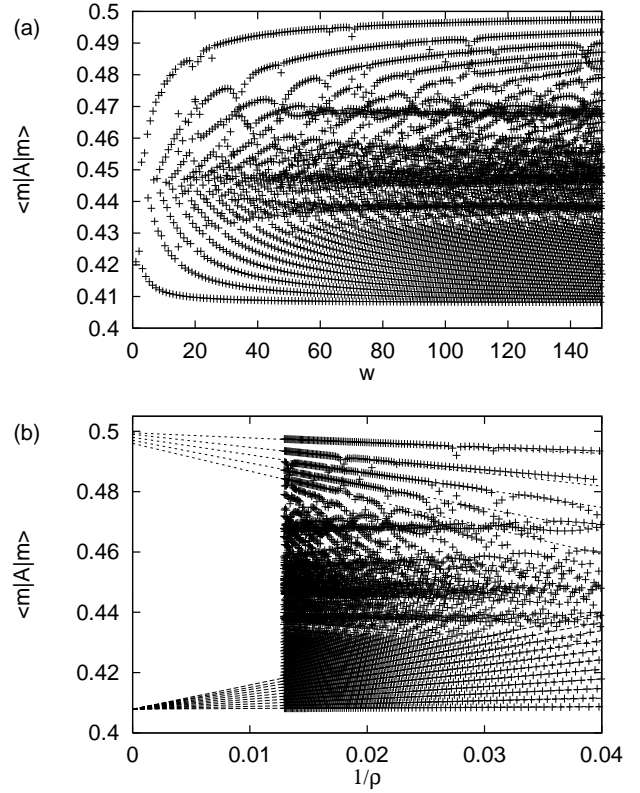


FIG. 4. Same as Fig. 2 but in the case of the scaled energy $\tilde{E} = -0.4$.

is done in Fig. 3b (resp. Fig. 4b) for the case $\tilde{E} = -0.316$ (resp. $\tilde{E} = -0.4$). In Fig. 3b, one sees that the three lower and the five upper dashed lines interpolating the values of the diagonal matrix elements as one goes towards the semiclassical limit have a common intersection. The value of the common intersection of the three lower sequences is very precisely equal to the limiting value $\langle \hat{A} \rangle_{r1} = \tau_{r1}/S_{r1} = 0.3933$ of the stable periodic orbit lying in the plane perpendicular to the direction of the magnetic field. The regular component which is therefore identified in a straightforward way. It is obviously the one to which the two conjugate central islands of stable motion of Fig. 1b are pertaining. As in the case $\tilde{E} = -0.2$, the three lower sequences are labelled by even values of the quantum number k , with the lowest sequence corresponding to $k = 0$. The value of the common intersection of the five upper sequences is very precisely equal to the limiting value $\langle \hat{A} \rangle_{r2} = \tau_{r2}/S_{r2} = 0.4136$ of the other stable periodic orbit. Consequently, the regular component which is associated to these sequences is the one whose fingerprint in Fig. 1b is constituted by the two conjugate chains of four islands of stable motion. Since this other orbit has no symmetry with respect to the plane perpendicular to the direction of the magnetic field, the five upper sequences are labelled by both even and odd values of the quantum number k , with the uppermost sequence corresponding to $k = 0$. Similar results are obtained in

the case $\tilde{E} = -0.4$. Indeed, one sees in Fig. 4b that the groups of dashed interpolating lines corresponding to the sequences above and below the statistical distribution have each a common intersection. The value of the common intersection of the sequences below the statistical distribution is very precisely equal to the limiting value $\langle \hat{A} \rangle_{r1} = \tau_{r1}/S_{r1} = 0.408$ of the stable periodic orbit lying in the plane perpendicular to the direction of the magnetic field. The regular component connected to these sequences is, as in the two previous cases, the one to whom the two conjugate islands of stable motion in the Poincaré surface of section are belonging. This means that the limiting value of a group of sequences readjusts itself to the change in length of the associated orbit as one moves from a particular example of the mixed phase-space to another. The sequences below the statistical distribution are labelled by even values of k , with the lowest sequence corresponding to $k = 0$. As expected, the value of the common intersection of the sequences above the statistical distribution is (nearly) equal to the limiting value $\langle \hat{A} \rangle_{r2} = \tau_{r2}/S_{r2} = 0.500$ of the stable periodic orbit which is parallel to the direction of the magnetic field. By way of consequence, the regular component which is linked to these sequences is the one whose fingerprint in Fig. 1c is the central island of stable motion. These sequences are labelled by both even and odd values of k , with the uppermost sequence corresponding to $k = 0$. Finally, the formula in Eq. (22) giving the mean value which characterizes the complete distribution of diagonal matrix elements is generalized to the case of several regular components simply by adding as many weighted classical values $\langle \hat{A} \rangle_r$ as there are stable periodic orbits in the underlying classical dynamics.

IV. NON-DIAGONAL TRANSITION MATRIX ELEMENTS

This section studies the quantitative contributions of the ergodic and regular components of the mixed phase-space to the variance characterizing the distributions of non-diagonal transition matrix elements associated to the perturbing operator \hat{A} . This is done with the help of scaled spectral functions which take the different types of non-diagonal transition matrix elements into account, those coupling chaotic or regular eigenstates together as well as those coupling a chaotic and a regular eigenstate together. Since they deal with non-diagonal matrix elements, these scaled spectral functions depend necessarily on two energy scales, the scaled energy w and the scaled energy difference Δw . The scaled total spectral function $C(w, \Delta w)$ is defined to be the sum of these scaled spectral functions, i.e.,

$$C(w, \Delta w) = C_{cc}(w, \Delta w) + C_{rr}(w, \Delta w) + C_{cr}(w, \Delta w) + C_{rc}(w, \Delta w) \quad (23)$$

with

$$C_{\alpha\beta}(w, \Delta w) = \sum_{m_\alpha, n_\beta} |\langle m_\alpha | \hat{A} - \langle \hat{A} \rangle_\alpha \delta_{\alpha\beta} | n_\beta \rangle|^2 \delta_\eta \left(w - \frac{w_m^{(\alpha)} + w_n^{(\beta)}}{2} \right) \times \delta_\epsilon \left(\Delta w - (w_n^{(\beta)} - w_m^{(\alpha)}) \right) \quad (24)$$

and $\alpha = c, r$; $\beta = c, r$. The (Lorentzian) smoothings of the δ -functions, of widths η and ϵ , are introduced so that one can compute these spectral functions in practice in spite of the discreteness of the spectrum. The values of the widths which have been chosen for the numerical computations are $\eta = 5.0$ and $\epsilon = 0.02$, in units of the scaling parameter w . The classical values $\langle \hat{A} \rangle_c, \langle \hat{A} \rangle_r$ are subtracted from the appropriate spectral functions in order to eliminate the quantitative contribution of the diagonal matrix elements in the semiclassical regime. The local variance $\sigma_c^2(w, \Delta w)$ which is associated to the statistical distributions of non-diagonal matrix elements coupling chaotic eigenstates together is related to the spectral function $C_{cc}(w, \Delta w)$ and to the mean density of states $\rho_{0,c}(w)$ by the formula [8]

$$\sigma_c^2(w, \Delta w) = \frac{C_{cc}(w, \Delta w)}{(\rho_{0,c}(w))^2}. \quad (25)$$

By analogy with this formula, the local variance $\sigma_t^2(w, \Delta w)$ which is associated to the distributions of all non-diagonal matrix elements is defined through the expression

$$\sigma_t^2(w, \Delta w) = \frac{C(w, \Delta w)}{(\rho_{0,t}(w))^2}. \quad (26)$$

The quantitative contribution of each spectral function in Eq. (23) to the variance $\sigma_t^2(w, \Delta w)$ is studied in the sequel.

The spectral function $C_{cc}(w, \Delta w)$ (resp. $C_{rr}(w, \Delta w)$) is connected to the regular (resp. ergodic) component of phase-space in a manner which is detailed below. On the contrary, the spectral functions $C_{cr}(w, \Delta w)$ and $C_{rc}(w, \Delta w)$ cannot be associated to a particular component of phase-space since they take both chaotic and regular eigenstates into account. According to Refs. [20,21], the quantitative contributions of these two last spectral functions to $C(w, \Delta w)$ should therefore be significantly smaller than those of the two first spectral functions. Fig. 5 shows that this is indeed the case in practice. This figure displays the distribution of values of the transition probabilities $|\langle n | \hat{A} | m \rangle|^2$ from a given initial state $|n\rangle$ to a subset $|m\rangle$ of final eigenstates corresponding to a finite range of the energy spectrum at scaled energy $\tilde{E} = -0.2$. In Fig. 5a, the chosen eigenstate $|n\rangle$ (the 575th state above the groundstate) is a regular eigenstate with $k = 0$ and eigenvalue $w_n^{(r)} \simeq 38.5$. On the contrary, the eigenstate $|n\rangle$ in Fig. 5b (the 944th state above the groundstate) is a chaotic eigenstate. In both figures, the diamonds (resp. crosses) are recording the values of the

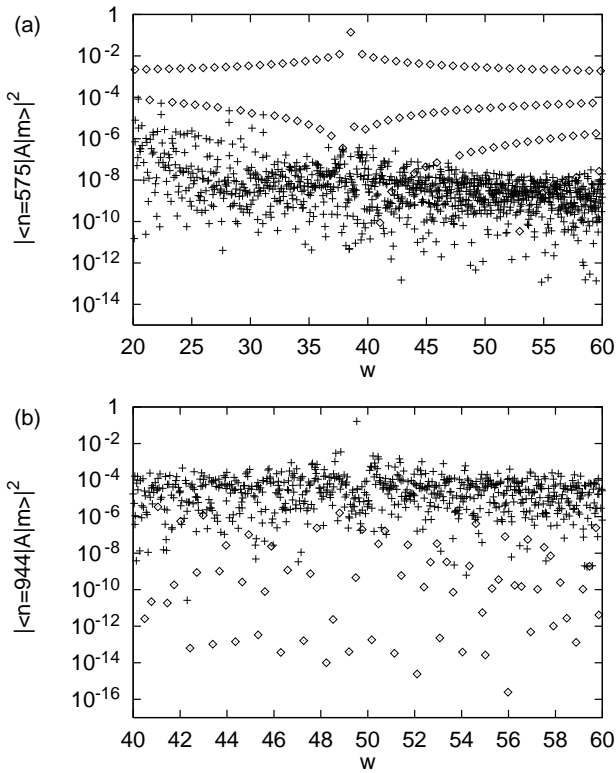


FIG. 5. Distribution of values of the transition probabilities $|\langle n|\hat{A}|m\rangle|^2$ as a function of the scaling parameter w in the case of the scaled energy $\tilde{E} = -0.2$. (a) Regular eigenstate $|n\rangle$; (b) Chaotic eigenstate $|n\rangle$. The diamonds and crosses mark the transitions to regular and chaotic states $|m\rangle$, respectively.

transition probabilities when the final eigenstate $|m\rangle$ is a regular (resp. chaotic) one. Each of the three visible sequences of diamonds in Fig. 5a is associated to regular eigenstates which are labelled by the same (even) value of k , with the uppermost sequence corresponding to $k = 0$. This figure shows clearly that the probabilities of most transitions coupling regular eigenstates together are several orders of magnitude larger than those coupling regular and chaotic eigenstates together. This implies in return that the values of the spectral function $C_{rr}(w, \Delta w)$ are much larger than those of the spectral functions $C_{rc}(w, \Delta w)$ and $C_{cr}(w, \Delta w)$. Two other observations in Fig. 5a are of interest. The first is that the square of the diagonal matrix element $\langle n = 575|\hat{A}|n = 575\rangle$ is at least one order of magnitude larger than the probabilities of transitions coupling different regular eigenstates together. The second observation is that the probabilities of the transitions involving regular eigenstates with the same value of k are more than one order of magnitude larger than those involving regular eigenstates with different values of k . Moreover, the larger the difference in k between two regular eigenstates, the smaller the corresponding transition probability [34]. It has also been checked that the values of the transition probabilities belonging to the sequence of diamonds with $k = 0$

are decaying exponentially as one goes away from the diagonal matrix element. This type of decay is a universal feature of one-dimensional systems [36]. The system behaves therefore as an effective one-dimensional system at the level of the transition amplitudes which are connected to the first quantized torus surrounding the stable orbit. Fig. 5b shows clearly that the probabilities of most transitions involving chaotic eigenstates are also several orders of magnitude larger than those involving chaotic and regular eigenstates. As a consequence, the values of the spectral function $C_{cc}(w, \Delta w)$ are also much larger than those of the spectral functions $C_{rc}(w, \Delta w)$ and $C_{cr}(w, \Delta w)$. The quantitative contribution of the two last spectral functions to the variance $\sigma_t^2(w, \Delta w)$ is therefore negligible.

As shown in Refs. [8,9], the leading order contribution to the spectral function $C_{cc}(w, \Delta w)$ is proportional to the Fourier transform of the classical autocorrelation function of the Weyl transform of the perturbing operator. By virtue of the ergodic theorem, the microcanonical average over the ergodic part of the energy shell appearing in the leading order contribution can be replaced with a time (i.e. scaled action) average along any ergodic trajectory exploring this part in a uniform way. The resulting expression of the leading order contribution to the local variance $\sigma_c^2(w, \Delta w)$ is [12]

$$\sigma_c^2(w, \Delta w) = \frac{1}{\pi \rho_{0,c}(w)} \text{Re} \int_0^\infty d\tilde{s} e^{i(\Delta w + i\epsilon)\tilde{s}} C_{\tilde{A},c}(\tilde{s}). \quad (27)$$

Here $C_{\tilde{A},c}(\tilde{s})$ is the classical autocorrelation function of the Weyl transform $\tilde{A}(\tilde{s})$, as computed along an ergodic trajectory of arbitrary large scaled action S , i.e.,

$$C_{\tilde{A},c}(\tilde{s}) = \lim_{S \rightarrow \infty} \frac{1}{S} \int_0^S d\tilde{s}' \times \left(\tilde{A}(\tilde{s}' + \tilde{s}/2) - \langle \hat{A} \rangle_c \right) \left(\tilde{A}(\tilde{s}' - \tilde{s}/2) - \langle \hat{A} \rangle_c \right). \quad (28)$$

The ergodic theorem ensures that the limit on the r.h.s. of this equation is well defined and unique. The appearance in Eq. (27) of a damping factor containing the width ϵ is a consequence of the smoothing of the δ -function which is associated to differences in scaled energies in Eq. (24). The formula in Eq. (27) is well suited for the numerical computation of the classical contribution to the local variance $\sigma_c^2(w, \Delta w)$. It shows that, at the level of the leading order contribution, the rescaled variance $\sigma_c^2(w, \Delta w)\rho_{0,c}(w)$ is a function which depends only on the scaled energy difference Δw and no more on the scaled energy w .

As a first numerical study, it is interesting to compare the values of the rescaled variances $\sigma_t^2(w, \Delta w)\rho_{0,t}(w)$ and $\sigma_c^2(w, \Delta w)\rho_{0,c}(w)$ over a large range of values of the scaled energy difference. This is done in Fig. 6 for the case $\tilde{E} = -0.2$. The full (resp. dashed) curve corresponds to the first (resp. second) rescaled variance. One sees that both curves are modulated by the period S_r of the stable

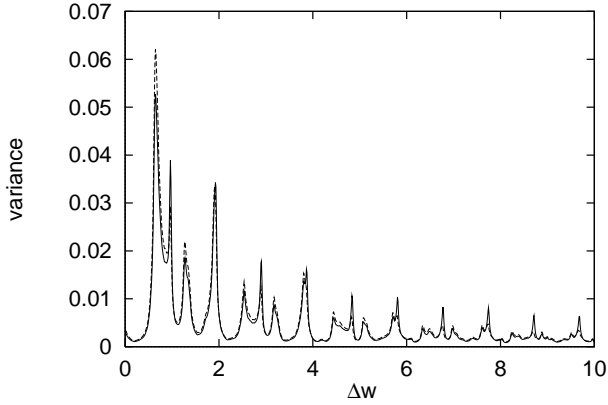


FIG. 6. Rescaled variances of the distributions of non-diagonal transition matrix elements as a function of the scaled energy difference Δw in the case of the scaled energy $\tilde{E} = -0.2$. Solid line: $\sigma_t^2(w, \Delta w)\rho_{0,t}(w)$; Dashed line: $\sigma_c^2(w, \Delta w)\rho_{0,c}(w)$.

orbit lying in the plane perpendicular to the direction of the magnetic field since they exhibit peaks exactly at the integer multiples of the value $\Delta w = 2\pi/S_r = 0.968$. This modulation effect of the local variance was already pointed out in Refs. [12,11]. One observes also that the two curves are only slightly different from each other. This observation simply reflects the fact that the number of transitions involving chaotic eigenstates is very much larger than the number of transitions involving regular eigenstates in the chosen example. Consequently, a numerical analysis using the bare variances themselves would not allow to get precise enough values for the quantitative contribution to the total variance coming from the regular part of phase-space. As seen below, it is necessary to use the Fourier transform of the rescaled variances in order to extract quantitative precise results from the numerical data. In practice, the full curve in Fig. 6 has been calculated with the help of the numerical data built up from the distributions of the non-diagonal matrix elements whereas the dashed curve has been computed by using Eqs. 27, 28. It is therefore interesting to compare the predictions of the expression of the leading order contribution to the local variance $\sigma_c^2(w, \Delta w)$ with the numerical values obtained from the distributions of non-diagonal matrix elements coupling chaotic eigenstates together. This is done in Fig. 7a for the case $\tilde{E} = -0.2$ and in Fig. 8a for the case $\tilde{E} = -0.316$. In both figures, the full curve represents the Fourier transform $C(S)$ of the rescaled variance $\sigma_c^2(w, \Delta w)\rho_{0,c}(w)$, i.e.,

$$C(S) = e^{\epsilon S} \int_{-\infty}^{+\infty} d(\Delta w) \cos(\Delta w S) \sigma_c^2(w, \Delta w) \rho_{0,c}(w), \quad (29)$$

as calculated from the relevant numerical data. On the other hand, the dashed curve represents the classical autocorrelation function $C_{\tilde{A},c}(S)$, Eq. (28), as computed

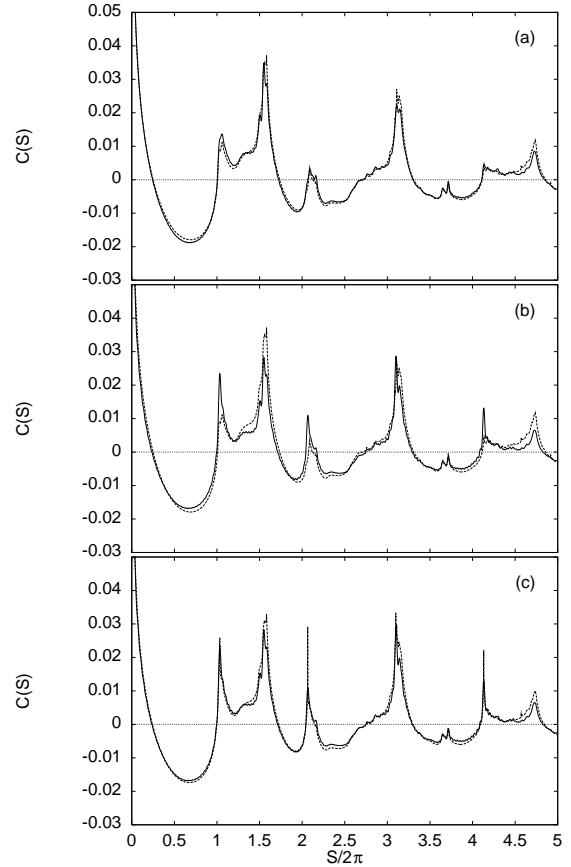


FIG. 7. Fourier transform of the rescaled variances of the distributions of non-diagonal transition matrix elements as a function of the scaled action $S/2\pi$ in the case of the scaled energy $\tilde{E} = -0.2$. (a) Solid line: Fourier transform of $\sigma_c^2(w, \Delta w)\rho_{0,c}(w)$; Dashed line: Autocorrelation function $C_{\tilde{A},c}$. (b) Solid line: Fourier transform of $\sigma_t^2(w, \Delta w)\rho_{0,t}(w)$; Dashed line: Autocorrelation function $C_{\tilde{A},c}$. (c) Solid line: Fourier transform of $\sigma_t^2(w, \Delta w)\rho_{0,t}(w)$; Dashed line: Weighted sum of autocorrelation functions $C_{\tilde{A},c}$ and $C_{\tilde{A},r}$.

along an arbitrary ergodic trajectory. Eq. (27) predicts that both curves are identical, i.e. $C(S) = C_{\tilde{A},c}(\tilde{S})$. Figs. 7a and 8a show that they agree well with each other over the whole range of values of the scaled action S . The values of the local variance $\sigma_c^2(w, \Delta w)$ can therefore be reproduced with an excellent precision by the leading order contribution alone.

The expression of the spectral function $C_{rr}(w, \Delta w)$ in the semiclassical regime is obtained much in the same way as the expression of the spectral function $D_r(w)$, Eq. (20). Indeed, the contribution of a stable periodic orbit and all its repetitions to $C_{rr}(w)$ has an expression which is analogous to the one given in Eq. (19). The only difference is that the amplitude A_r is now replaced with the Fourier transform of the autocorrelation function of the Weyl transform of the perturbing operator along the stable periodic orbit [8,9,11]. The formal resummation of all contributions leads to the semiclassical expression

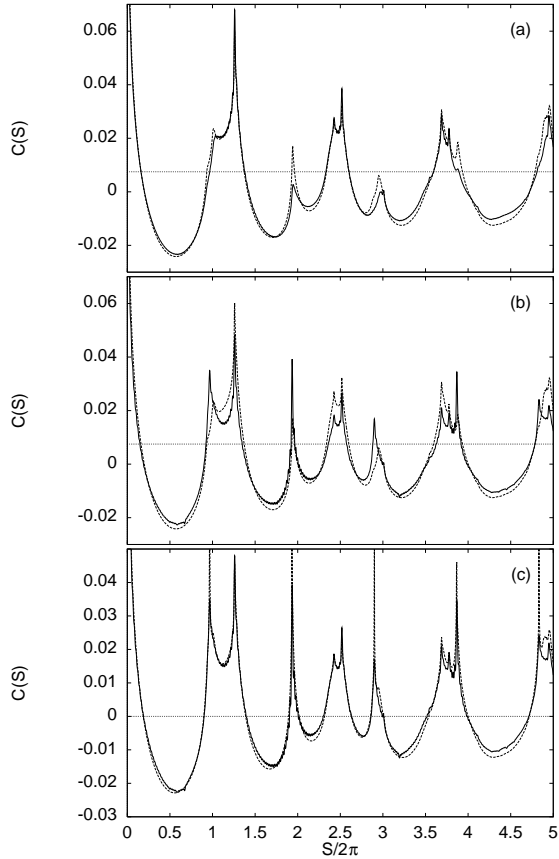


FIG. 8. Same as Fig. 7 but in the case of the scaled energy $\tilde{E} = -0.316$.

$$C_{rr}(w, \Delta w) = \frac{\rho_{0,r}(w)}{\pi} \text{Re} \int_0^\infty d\tilde{s} e^{i(\Delta w + i\epsilon)\tilde{s}} C_{\tilde{A},r}(\tilde{s}), \quad (30)$$

with the autocorrelation function $C_{\tilde{A},r}(\tilde{s})$ given by

$$C_{\tilde{A},r}(\tilde{s}) = \frac{1}{S_r} \oint d\tilde{s}' \times \left(\tilde{A}(\tilde{s}' + \tilde{s}/2) - \langle \hat{A} \rangle_r \right) \left(\tilde{A}(\tilde{s}' - \tilde{s}/2) - \langle \hat{A} \rangle_r \right). \quad (31)$$

The autocorrelation function is a periodic function with the same period S_r as the one of the orbit [8,11]. In order to check the validity of the semiclassical expression of $C_{rr}(w, \Delta w)$, it is easier to take the Fourier transform with respect to the scaled energy difference Δw on both sides of Eq. (30) and to integrate subsequently with respect to the scaled energy w . If N is the number of regular states in the used spectrum, one gets the following expression of the autocorrelation function

$$C_{\tilde{A},r}(S) = \frac{1}{N} \sum_{m_r, n_r} |\langle m_r | \hat{A} - \langle \hat{A} \rangle_r | n_r \rangle|^2 \times \cos \left(\left(w_m^{(r)} - w_n^{(r)} \right) S \right). \quad (32)$$

Fig. 9 compares the values of the autocorrelation function, as computed with the help of Eq. (32) (full curve)

and Eq. (31) (dashed curve). The comparison is done in the case $\tilde{E} = -0.2$ ($N = 120$) and over one period of the stable trajectory. It is seen that the agreement between both curves is good, except in the vicinity of the values $S = 0$ and $S = S_r$ for which the expression in Eq. (31) is singular. The full curve would reproduce this singular behavior all the better as the number of regular states used in the computation would be larger. The finite number of regular states is also responsible for the observed little discrepancies between both curves in the considered interval of values of the scaled action. In spite of these discrepancies, the general good agreement between the full and the dashed curve allows to conclude that the semiclassical expression given in Eq. (30) can be used to calculate the values of the spectral function $C_{rr}(w, \Delta w)$. By analogy with Eq. (25), one can also introduce a local variance $\sigma_r^2(w, \Delta w)$ corresponding to the distributions of non-diagonal matrix elements coupling regular eigenstates together, defined as

$$\sigma_r^2(w, \Delta w) = \frac{C_{rr}(w, \Delta w)}{(\rho_{0,r}(w))^2}. \quad (33)$$

It is to be noted that the spectral functions which are associated to the distributions of non-diagonal matrix elements involving chaotic (Eqs. 27, 28) and regular (Eqs. 30, 31) states have similar classical expressions. As in the case of the diagonal matrix elements, each expression takes into account the classical trajectory which is related to the component of phase-space connected to the studied subset of non-diagonal matrix elements.

It has been checked previously that a very close estimate of the values of the total spectral function $C(w, \Delta w)$ is obtained through the sum of the two spectral functions $C_{cc}(w, \Delta w)$ and $C_{rr}(w, \Delta w)$. Consequently, by virtue of Eqs. 26, 25 and 33, the rescaled variance which is associated to the distributions of all non-diagonal matrix elements can be written as

$$\sigma_t^2(w, \Delta w) \rho_{0,t}(w) = \left(\frac{\rho_{0,c}(w)}{\rho_{0,t}(w)} \right) \sigma_c^2(w, \Delta w) \rho_{0,c}(w) + \left(\frac{\rho_{0,r}(w)}{\rho_{0,t}(w)} \right) \sigma_r^2(w, \Delta w) \rho_{0,r}(w). \quad (34)$$

As in the case of the mean value $\langle \hat{A} \rangle_t$, Eq. (22), the contribution to the rescaled variance $\sigma_t^2(w, \Delta w) \rho_{0,t}(w)$ of the ergodic (resp. regular) component of phase-space is weighted by the ratio of the mean density of states of the subset of chaotic (resp. regular) states to the mean total density of states. Equivalently, taking the Fourier transform on both sides of Eq. (34) with respect to the scaled energy difference Δw , one obtains the following formula with the help of Eqs. 27, 30 and 33

$$e^{\epsilon S} \int_{-\infty}^{+\infty} d(\Delta w) \cos(\Delta w S) \sigma_t^2(w, \Delta w) \rho_{0,t}(w) = \left(\frac{\rho_{0,c}(w)}{\rho_{0,t}(w)} \right) C_{\tilde{A},c}(S) + \left(\frac{\rho_{0,r}(w)}{\rho_{0,t}(w)} \right) C_{\tilde{A},r}(S). \quad (35)$$

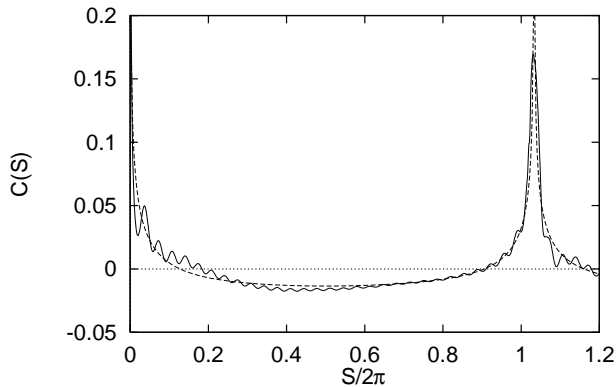


FIG. 9. Autocorrelation function $C_{\tilde{A},r}$ as a function of the scaled action $S/2\pi$ in the case of the scaled energy $\tilde{E} = -0.2$. Solid line: Computation with Eq. 32; Dashed line: Computation with Eq. 31.

The numerical comparison between both sides of this equation is done in Figs. 7b,c for the case $\tilde{E} = -0.2$. In Fig. 7b, the full curve represents the Fourier transform of the rescaled variance whereas the dashed curve represents the autocorrelation function $C_{\tilde{A},c}(S)$ alone. One sees that both curves do not agree so much with each other. One has to compare Fig. 7b with Fig. 7c in order to appreciate the quantitative improvement which is brought in the weighted sum by the contribution originating from the stable periodic orbit. In this last figure, the full curve represents again the Fourier transform of the rescaled variance whereas the dashed curve represents now the weighted sum of the autocorrelation functions on the r.h.s. of Eq. (35). Contrary to Fig. 7b, both curves agree now well with each other over the whole range of values of S . The improvement is especially noticeable in the immediate vicinity of the peaked structures located at positions which are multiple integers of $S_r/2\pi = 1.03305$. This is due to the fact that the autocorrelation function $C_{\tilde{A},r}(S)$ contributes mostly to the Fourier transform in the immediate vicinity of these positions, as shown by Fig. 9. Fig. 7c provides also another confirmation of the fact that the spectral functions $C_{cr}(w, \Delta w)$ and $C_{rc}(w, \Delta w)$ give really a negligible quantitative contribution to the local variance. One can therefore conclude that Eq. (34) is able to reproduce the values of the local variance with an excellent precision. This equation generalizes to the case of a scaled system with a mixed phase-space the expression of the local variance given in Refs. [8,9] for a scaled system with an ergodic phase-space. As in the case of the diagonal matrix elements, the generalization of Eq. (34) to a situation with several regular components in phase-space is straightforward. Indeed, one has to add as many weighted rescaled variances $\sigma_r^2(w, \Delta w)\rho_{0,r}(w)$ as there are stable periodic orbits in the underlying classical dynamics, as illustrated by the remaining figures. On the one hand, Fig. 8b (resp. Fig. 10a) compares the Fourier transform of the rescaled variance $\sigma_t^2(w, \Delta w)\rho_{0,t}(w)$ (full curve) with the autocorrelation function $C_{\tilde{A},c}(S)$ (dashed curve) in the case

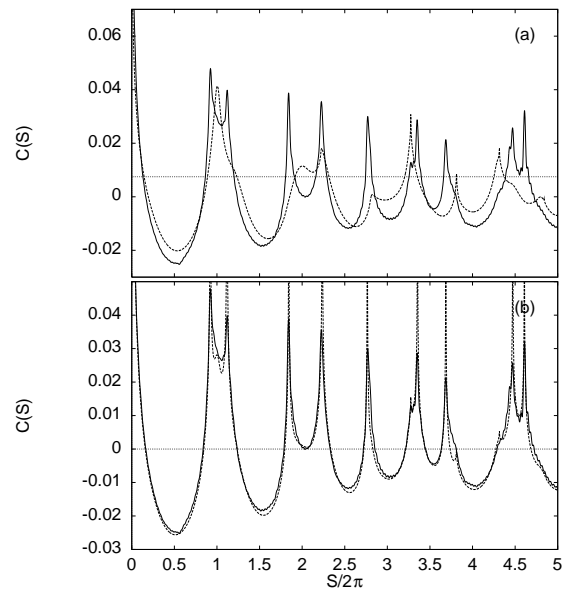


FIG. 10. Fourier transform of the rescaled variance $\sigma_t^2(w, \Delta w)\rho_{0,t}(w)$ of the distributions of non-diagonal transition matrix elements as a function of the scaled action $S/2\pi$ in the case of the scaled energy $\tilde{E} = -0.4$. (a) Solid line: Fourier transform of $\sigma_t^2(w, \Delta w)\rho_{0,t}(w)$; Dashed line: Autocorrelation function $C_{\tilde{A},c}$. (b) Solid line: Fourier transform of $\sigma_t^2(w, \Delta w)\rho_{0,t}(w)$; Dashed line: Weighted sum of autocorrelation functions $C_{\tilde{A},c}$ and $C_{\tilde{A},r}$.

$\tilde{E} = -0.316$ (resp. $\tilde{E} = -0.4$). As in the previous case, there are many discrepancies between both curves because the contributions coming from the stable periodic orbits are missing. On the other hand, Fig. 8c (resp. Fig. 10b) compares the Fourier transform of the rescaled variance (full curve) with the weighted sum of autocorrelation functions (dashed curve) in the case $\tilde{E} = -0.316$ (resp. $\tilde{E} = -0.4$). The sum now contains the properly weighted contributions originating from the stable periodic orbits which have been identified in the previous Section. In both cases, the very good agreement between the two curves confirms the validity of the generalization of Eq. (34).

V. CONCLUSION

This paper has been devoted to the study of the quantitative contributions of the different components making up a mixed phase-space to the value of the mean characterizing the distribution of diagonal transition matrix elements and to the value of the variance characterizing the distributions of non-diagonal transition matrix elements. With the help of numerical computations done in the framework of the Hydrogen atom in a strong magnetic field, it has been shown that these contributions can be well identified in the semiclassical regime. The computations have confirmed that the leading order contribution of the ergodic component to the mean is equal to the

average of the Weyl transform \tilde{A} of the perturbing operator A along an arbitrary ergodic trajectory. They have also confirmed that the leading order contribution of the same component to the variance is proportional to the Fourier transform of the autocorrelation function of \tilde{A} , this autocorrelation function being also computed along an arbitrary ergodic trajectory. On the other hand, it has been found that the contribution of each regular component to the mean is equal to the average of A around the corresponding stable orbit. It has also been found that the contribution of each such component to the variance is proportional to the Fourier transform of the autocorrelation function of \tilde{A} , this autocorrelation function being again computed around the corresponding stable orbit. For each studied quantity, the contributions coming from the ergodic and regular components have therefore similar expressions, each expression taking into account the particular classical trajectory which is related to the considered component. The stable periodic orbits provide a convenient method to compute the contributions of the various regular components to mean and variance with high accuracy. This method is different from the one which has been proposed by Robnik and Prosen for the same purpose. As a final step, it has been shown that mean and variance can be expressed as a weighted sum of the contributions of all different components belonging to the mixed phase-space. The weight appearing in front of a given contribution has been identified as the ratio of the mean density of states of the corresponding component to the mean total density of states of the system. Although the study has been done for a particular scaling system, the results presented in this paper are relevant to all generic scaling systems with a small number of degrees of freedom having a mixed phase-space.

ACKNOWLEDGMENTS

We thank B. Mehlig and K. Müller for discussions and a referee for useful comments. This work was supported in part by the Deutsche Forschungsgemeinschaft (Sonderforschungsbereich No. 237).

-
- [1] O. Bohigas, in : *Chaos and Quantum Physics, Les Houches 1989, Session LII*, ed. by M. J. Giannoni, A. Voros, and J. Zinn-Justin (North-Holland, Amsterdam, 1990), 87.
- [2] J. J. M. Verbaarschot, H. A. Weidenmüller, and M. R. Zirnbauer, *Phys. Rep.* **129**, 367 (1985).
- [3] M. V. Berry, in : *Chaos and Quantum Physics, Les Houches 1989, Session LII*, ed. by M. J. Giannoni, A. Voros, and J. Zinn-Justin (North-Holland, Amsterdam, 1990), 251.
- [4] U. Smilansky, in : *Chaos and Quantum Physics, Les Houches 1989, Session LII* ed. by M. J. Giannoni, A. Voros, and J. Zinn-Justin (North-Holland, Amsterdam, 1990), 371.
- [5] C. E. Porter, *Statistical Theories of Spectra: Fluctuations* (Academic, New York, 1965).
- [6] M. C. Gutzwiller, *J. Math. Phys.* **8**, 1979 (1967); **10**, 1004 (1969); **11**, 1791 (1970); **12**, 343 (1971).
- [7] M. C. Gutzwiller, *Chaos in Classical and Quantum Mechanics* (Springer, New York, 1990).
- [8] M. Wilkinson, *J. Phys. A* **20**, 2415 (1987); **21**, 1173 (1988); see also M. Feingold and A. Peres, *Phys. Rev. A* **34**, 591 (1986).
- [9] B. Eckhardt, S. Fishman, K. Müller, and D. Wintgen, *Phys. Rev. A* **45**, 3531 (1992).
- [10] E. J. Austin and M. Wilkinson, *Europhys. Lett.* **20**, 589 (1992).
- [11] B. Mehlig, D. Boosé, and K. Müller, *Phys. Rev. Lett.* **75**, 57 (1995).
- [12] D. Boosé, J. Main, B. Mehlig, and K. Müller, *Europhys. Lett.* **32**, 295 (1995).
- [13] B. Mehlig, *Phys. Rev. B* **55**, R10193 (1997).
- [14] E. B. Bogomolny and J. P. Keating, *Phys. Rev. Lett.* **77**, 1472 (1996).
- [15] A. V. Andreev and B. L. Altshuler, *Phys. Rev. Lett.* **75**, 902 (1995).
- [16] M. V. Berry and M. Robnik, *J. Phys. A* **17**, 2413 (1984).
- [17] T. H. Seligman and J. J. M. Verbaarschot, *J. Phys. A* **18**, 2227 (1985).
- [18] T. A. Brody, *Lett. Nuovo Cimento* **7**, 482 (1973).
- [19] F. M. Izrailev, *Phys. Lett. A* **125**, 250 (1987); **134**, 13 (1988).
- [20] T. Prosen and M. Robnik, *J. Phys. A* **26**, L319 (1993).
- [21] T. Prosen, *Ann. Phys. N.Y.* **235**, 115 (1994).
- [22] A. Voros, in : *Colloques Internationaux CNRS 237* (1975), 277.
- [23] W. H. Miller, *J. Chem. Phys.* **63**, 996 (1975).
- [24] D. Boosé and J. Main, *Phys. Lett. A* **217**, 253 (1996).
- [25] H. Friedrich and D. Wintgen, *Phys. Rep.* **183**, 37 (1989).
- [26] D. Wintgen, K. Richter, and G. Tanner, *CHAOS* **2**, 19 (1992).
- [27] A. Holle, J. Main, G. Wiebusch, H. Rottke, and K. H. Welge, *Phys. Rev. Lett.* **61**, 161 (1988); J. Main, G. Wiebusch, and K. H. Welge, *Commun. At. Mol. Phys.* **25**, 233 (1991).
- [28] J. Main, G. Wiebusch, K. H. Welge, J. Shaw, and J. B. Delos, *Phys. Rev. A* **49**, 847 (1994).
- [29] J. Main and G. Wunner, *J. Phys. B* **27**, 2835 (1994).
- [30] T. Ericsson and A. Ruhe, *Math. Comp.* **35**, 1251 (1980).
- [31] D. Wintgen and H. Friedrich, *Phys. Rev. A* **36**, 131 (1987).
- [32] K. Müller and D. Wintgen, *J. Phys. B* **27**, 2693 (1994).
- [33] Eq. (1) of Ref. [24] does not give the accurate expression of the microcanonical average. One obtains the accurate expression by replacing the scaling parameter (which is called z in Ref. [24]) by the scaled energy \tilde{E} in the numerator and denominator of Eq. (1).
- [34] I. C. Percival, *Adv. Chem. Phys.* **36**, 1 (1977).
- [35] O. Bohigas, S. Tomsovic, and D. Ullmo, *Phys. Rep.* **223**, 43 (1993).
- [36] L. D. Landau and E. M. Lifshitz, *Quantum Mechanics* (Pergamon Press, London - Paris, 1959), §51.